



## Coordinate sizing of energy storage and transmission line for a remote renewable power plant

Xie, Rui; Wei, Wei; Ge, Ming-Feng; Wu, Qiuwei; Mei, Shengwei

*Published in:*  
IET Renewable Power Generation

*Link to article, DOI:*  
[10.1049/rpg2.12440](https://doi.org/10.1049/rpg2.12440)

*Publication date:*  
2022

*Document Version*  
Publisher's PDF, also known as Version of record

[Link back to DTU Orbit](#)

*Citation (APA):*  
Xie, R., Wei, W., Ge, M.F., Wu, Q., & Mei, S. (2022). Coordinate sizing of energy storage and transmission line for a remote renewable power plant. *IET Renewable Power Generation*, 16(12), 2508-2520.  
<https://doi.org/10.1049/rpg2.12440>

---

### General rights

Copyright and moral rights for the publications made accessible in the public portal are retained by the authors and/or other copyright owners and it is a condition of accessing publications that users recognise and abide by the legal requirements associated with these rights.

- Users may download and print one copy of any publication from the public portal for the purpose of private study or research.
- You may not further distribute the material or use it for any profit-making activity or commercial gain
- You may freely distribute the URL identifying the publication in the public portal

If you believe that this document breaches copyright please contact us providing details, and we will remove access to the work immediately and investigate your claim.

## ORIGINAL RESEARCH

# Coordinate sizing of energy storage and transmission line for a remote renewable power plant

Rui Xie<sup>1</sup>  | Wei Wei<sup>1</sup> | Ming-Feng Ge<sup>2</sup>  | Qiuwei Wu<sup>3</sup> | Shengwei Mei<sup>1</sup>
<sup>1</sup>State Key Laboratory of Power Systems,  
Department of Electrical Engineering, Tsinghua  
University, Beijing, China

<sup>2</sup>School of Mechanical Engineering and Electronic  
Information, China University of Geosciences,  
Wuhan, China

<sup>3</sup>Center for Electric Power and Energy, Technical  
University of Denmark, Kongens Lyngby, Denmark

## Correspondence

Wei Wei, State Key Laboratory of Power Systems,  
Department of Electrical Engineering, Tsinghua  
University, 100084 Beijing, China.  
Email: wei-wei04@mails.tsinghua.edu.cn

## Funding information

National Natural Science Foundation of China,  
Grant/Award Numbers: 51807101, U1766203

## Abstract

To protect the environment and reduce carbon emissions, renewable power generation has been growing rapidly during the past decade. Renewable energy resources are sometimes far away from the main grid, leading to expensive grid-connection transmission lines. Deploying on-site energy storage can smooth the output power and help to reduce the renewable power spillage and the requirement of transmission line capacity. This paper presents a method to coordinately size on-site energy storage and grid-connection transmission line for a remote renewable power plant, minimising the total investment cost subject to the constraint of renewable curtailment risk. Through an optimal operation model, the renewable curtailment is proven to be a piecewise affine function of capacity parameters and renewable power generation, and a linear programming-based algorithm is proposed to generate an approximate expression. A distributionally robust optimisation model is proposed to determine the sizes. The renewable generation uncertainty is modelled by a Wasserstein-metric-based ambiguity set containing probability distributions around the empirical distribution constructed from the historical data. The utilisation rate is ensured in the worst-case distribution. The sizing problem is transformed into a tractable linear program. The case study demonstrates the effectiveness of the proposed method.

## 1 | INTRODUCTION

Using renewable energy resources for electricity generation helps to save fossil energy, reduce carbon dioxide emissions, and protect the environment [1]. The sharing of renewable generation has been increasing rapidly during the past decades. International Energy Agency (IEA) reports that from 1990 to 2019 the average annual growth rates of world photovoltaic (PV) and wind are 36.0% and 22.6%, respectively [2].

In some countries, renewable energy resources are far away from the load centre. For an instance, northwestern China is rich in solar and wind resources while the low population density there results in low power demand. The electricity is then transmitted to the eastern load centre [3]. Remote renewable power plants may arise in this situation. In fact, they are not rare, especially for large-scale renewable power

plants. To list a few, Bhadla Solar Park has a total capacity of 2,245 MW in India, which is located in a sandy, dry, and almost unliveable area, and the transmission system contains 765 and 400 kV double-circuit line [4]. In China's northwestern province Qinghai, Huanghe Hydropower has constructed a 2.2 GW solar plant equipped with storage, which is connected to an ultra-high voltage power line of 1,587 km [5]. Located in desert areas in Gansu, China, Jiuquan Wind Power Base is planned 20 GW in total, and a 750 kV AC power line is constructed to carry the electricity [6]. London Array is an offshore wind farm in the UK, where 220 km export cabling transmits the power to Cleve Hill [7]. Therefore, the considered remote renewable power plants are practical and exist around the world. Since they are far away from the existing power grid infrastructure, grid-connection transmission lines should be constructed in companion with the renewable power plant, causing additional investments.

This is an open access article under the terms of the [Creative Commons Attribution-NonCommercial-NoDerivs](https://creativecommons.org/licenses/by-nc-nd/4.0/) License, which permits use and distribution in any medium, provided the original work is properly cited, the use is non-commercial and no modifications or adaptations are made.

© 2022 The Authors. *IET Renewable Power Generation* published by John Wiley & Sons Ltd on behalf of The Institution of Engineering and Technology.

The output of PV and wind generation is volatile and uncertain, depending on the real-time weather conditions [8]. The average power generation is usually much lower than the nominal power. Therefore, the utilisation rate of a transmission line with the same capacity as the renewable plant is low. The energy storage system (ESS) can be equipped in the renewable power plant to smooth the output [9] and thus reduce the capacity of the transmission line. The benefit is twofold. First, the plant power becomes partially controllable and the main grid could face fewer uncertainties [10]; second, considering the long distance of transmission corridor, the cost of building unit capacity of ESS is typically much lower than that of building unit capacity of transmission line, so deploying on-site ESS may save a significant amount of investment. In this regard, the capacities of the transmission line and ESS should be jointly optimised.

There are some existing researches about the co-planning of transmission and energy storage in bulk power systems. The transmission expansion planning with batteries in a market-driven power system is investigated in ref. [11], where the batteries are shown to be beneficial for social welfare and delaying the construction of transmission lines. The interdependence of transmission and energy storage is studied in ref. [12] through a theoretical model, which reveals that storage and transmission can be complements or substitutes under different conditions such as location and congestion factors. From the perspective of transmission network incentive regulation, the impacts of energy storage on transmission planning are investigated in ref. [13]. A scenario-based method is proposed in ref. [14] for the coordinated planning of transmission and ESS against malicious attacks. Considering security constraints and reliability level, ref. [15] presents a co-planning model, which is linearised and decomposed to become solvable. A method is proposed in ref. [16] for the large-scale co-planning problem of compressed air energy storage and transmission network.

Energy storage can help to accommodate renewable energy. Some studies investigate the coordinated planning of transmission and ESS in power systems with high-penetration renewable energy. A co-planning model is proposed in ref. [17] considering the decisions of merchant storage owner, centralised transmission expansion, and market clearing. A mixed-integer linear program is established in [18] to plan the size, location, and time of transmission and ESS investments, where the renewable generation is modelled by historical data. Batteries and pumped energy storage are both considered in ref. [19], and the total cost including investment, operation, and risk of excessive wind curtailment is minimised. In refs. [20–22], power generation, transmission network, and energy storage are jointly planned to facilitate renewable energy accommodation. The method in ref. [20] also improves the load acceptance level. The uncertainties of renewable energy and load demand are modelled by representatives from clustering in refs. [21, 22], and ref. [22] adopts a Benders dual decomposition method for problem-solving. In ref. [23], the co-planning aims at improving the resilience against extreme weather events, where the forecast load is from

deep learning. The investments of battery energy storages and thyristor-controlled series compensators are combined with transmission expansion planning in ref. [24].

The coordinated planning problem has to deal with the uncertainties of renewable energy. In the literature mentioned above, stochastic programming (SP) is adopted to handle the optimisation problems containing uncertainties, in which the probability distribution of the random variables is assumed to be known, based on certain types of distributions, scenarios, or historical data. However, the exact probability distribution is difficult to procure; the empirical distribution obtained from limited historical data may be biased, leading to the underestimation of renewable curtailment rates.

To avoid the impact of inaccurate distribution, robust optimisation (RO) is developed, which considers the worst-case scenario of the random variables. It improves the robustness of the results against the inaccurate empirical distribution. In ref. [25], the worst-case scenario of load demand and wind power is considered in the transmission and energy storage expansion planning of wind power-integrated power systems, in which the investment cost, operation cost, and penalty for unserved load are minimised. In the robust co-planning model of ref. [26], binary variables are used to indicate the status of energy storage, and the model is solved by a nested column and constraint algorithm. Bernstein polynomial is adopted in ref. [27] to derive a continuous-time robust model with a polyhedral uncertainty set of wind power. However, the worst-case scenario of renewable energy generation is unlikely to happen due to the low probability. The trade-off between improving reliability and reducing conservativeness remains an open problem.

To make a good compromise between SP and RO, distributionally robust optimisation (DRO) has drawn attention these years, which considers the worst-case distribution in an ambiguity set of candidate distributions. The distance-based ambiguity set includes distributions near the empirical distribution, and it is promising to contain the real distribution if properly selected. Ref. [28] uses the ambiguity set based on Kullback–Leibler divergence for the coordinated planning of transmission line and ESS of a remote PV power plant. However, this kind of ambiguity set only consists of discrete distributions, which makes it not suitable for modelling renewable energy generation. Wasserstein-metric-based ambiguity set also contains other types of distributions such as continuous distributions, and it is valid even for a small amount of data. Ref. [29] uses Wasserstein metric to form the ambiguity set, and gives a conservative approximation utilising an estimated property of the renewable energy curtailment, but the impacts of renewable generation and capacity parameters on the curtailment are not accurately considered. Ref. [30] follows the same paradigm as ref. [29] to size energy storage in bulk power systems. Ref. [31] proposes a method to evaluate the impacts of capacities on curtailment through multiparametric programming, under given renewable generation.

There are also studies on the planning of various components besides energy storage in power systems. For instances of power grids, a mixed-integer linear programming approach is

proposed in ref. [32] to optimally site and size energy storage to minimise the costs. The power grid is analysed by complex network theory in ref. [33] and based on which the siting and sizing of energy storage are studied. A planning framework of energy storage considering frequency constraints is established in ref. [34]. The allocation of ESS in power grids is addressed in ref. [35] with a contingency-sensitivity-based heuristic method. In the case of microgrids, ref. [36] proposed a method to determine the site and size of diesel generators, solar panels, and batteries by a two-stage particle swarm optimisation algorithm. An optimal siting and sizing procedure for ESS in a military-based microgrid is proposed in ref. [37] based on stochastic programming. Ref. [38] focuses on the planning of battery ESS in hybrid AC/DC microgrids considering post-contingency corrective rescheduling, where stochastic programming and robust optimisation are used to deal with the uncertainties. For the planning problem in distribution systems, an algorithm is proposed for planning ESS to control voltage in ref. [39], where the worst cases are considered to determine the sizes. The planning problems of distributed generation units, electric vehicle charging stations, and energy storage systems in a distribution network are studied in ref. [40] based on second-order conic programming. Renewable generation and battery storage are coordinated planned in ref. [41] considering distribution transformer constraints.

This paper differs from the existing studies in terms of problem and methodology. This paper focuses on the capacity planning problem of energy storage and transmission line for a remote renewable power plant, intending to optimise the economy, including maintaining energy curtailment requirements and minimising total costs. To deal with the uncertainties of renewable generation and the inaccurate empirical distribution, distributionally robust optimisation based on the Wasserstein metric is adopted to form the sizing problem, and it is equivalently transformed into linear programming. The contribution is twofold.

- 1) A distributionally robust optimisation model for jointly sizing ESS and transmission line for a remote renewable power plant, aiming at reducing the transmission capacity so as to save investment; as a result, the uncertainty faced by the power grid is also alleviated. Meanwhile, the renewable curtailment requirement is described via a distributionally robust risk constraint based on Conditional Value-at-Risk (CVaR), taking the inexactness of empirical distribution into account. The proposed model achieves a high utilisation rate of renewable energy, investment cost saving, and uncertainty reduction at the same time.
- 2) A systematic method to solve the distributionally robust capacity sizing model. The key is to reformulate the distributionally robust curtailment constraint. To this end, the operation problem that minimises renewable curtailment is formulated as a multiparametric linear program with renewable generation and capacities being the parameters. A linear-programming-based procedure is developed to express the curtailment as an analytical piecewise affine function in the parameters. Then, the distributionally robust curtailment

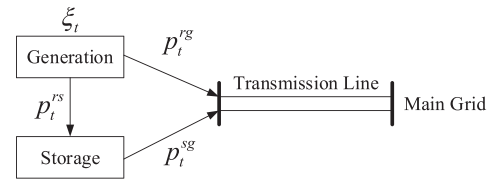


FIGURE 1 Energy flow

constraint is transformed into linear constraints through the property of CVaR. Finally, the distributionally robust capacity sizing problem comes down to a linear program and can be efficiently solved.

The rest of this paper is organised as follows. The distributionally robust capacity sizing problem is established in Section 2. The solution method is developed in Section 3. Case studies are presented in Section 4. The conclusion is drawn in Section 5.

## 2 | MATHEMATICAL FORMULATION

In this section, the operation problem is introduced first; then the ambiguity set of uncertain renewable power generation is presented, based on which the curtailment constraint is established; finally, the distributionally robust capacity sizing problem is formulated.

### 2.1 | Operation problem

The considered remote renewable power plant will be equipped with on-site ESS and connected to the main grid through a transmission line, where the energy flow is depicted in Figure 1. In the operation problem,  $T$  periods with duration  $\Delta_t$  are considered. The maximum output from the plant in period  $t$  is  $\xi_t$  which is uncertain, and  $p_t^c$  denotes the curtailment. The power from generation to storage, from generation to transmission, and from storage to transmission in period  $t$  are denoted by  $p_t^{rs}$ ,  $p_t^{rg}$ , and  $p_t^{sg}$ , respectively.

Let  $x_p$ ,  $x_e$ , and  $x_l$  denote the ESS power capacity, ESS energy capacity, and transmission line capacity, respectively. The energy storage level at the end of period  $t$  is  $e_t$ , and the initial storage level is  $e_0$ , then the operation problem is cast as

$$f(x, \xi) := \min \sum_t p_t^c \Delta_t \quad (1a)$$

$$\text{s.t. } p_t^{rs}, p_t^{rg}, p_t^{sg}, p_t^c \geq 0, \forall t \quad (1b)$$

$$\xi_t^g = p_t^{rs} + p_t^{rg} + p_t^c, \forall t \quad (1c)$$

$$p_t^{rg} + p_t^{sg} \leq x_l, \forall t \quad (1d)$$

$$e_t = e_0 + \sum_{s=1}^t \left( \eta_c p_s^{rs} - \frac{p_s^{sg}}{\eta_d} \right) \Delta_t, \forall t \quad (1e)$$

$$\omega_l x_c \leq e_t \leq \omega_h x_c, e_T = e_0, \forall t \quad (1f)$$

$$\dot{p}_t^{rs} \leq x_p, \dot{p}_t^{sg} \leq x_p, \forall t \quad (1g)$$

$$\dot{p}_t^{rs} + \dot{p}_t^{sg} \leq x_p, \forall t \quad (1h)$$

where the objective function (1a) is to minimise the total renewable energy curtailment; constraint (1b) stipulates the power flow direction and the non-negativity of variables; constraint (1c) represents the power balance at the generation side; (1d) is the capacity constraint of the transmission line; constraints (1e)–(1h) compose the ESS operation model [42], where  $\eta_c$  and  $\eta_d$  are charging and discharging efficiencies of the ESS, respectively, and Equation (1e) depicts the storage dynamics;  $\omega_l$  and  $\omega_h$  are the lower and upper bounds of the ESS state of charge (SoC), respectively, and Equation (1f) contains the bounds for stored energy and equal initial and terminal stored energy for continuous operation; there are the upper bounds for charging and discharging power in Equation (1g); Equation (1h) allows a time period to be divided into a charging subinterval and a discharging subinterval, and the charging power and discharging power, if not strictly complement, are still physically implementable [42]: for example, regard  $\dot{p}_t^{rs}$  and  $\dot{p}_t^{sg}$  as average power in period  $t$ ; charge the ESS with power  $x_p$  first for  $\dot{p}_t^{rs} \Delta_t / x_p$  time, after that discharge ESS with power  $x_p$  for  $\dot{p}_t^{sg} \Delta_t / x_p$  time, and do not charge or discharge in the remaining time of period  $t$ . So there is no need to charge and discharge the ESS simultaneously.

In the operation problem (1), the capacities  $x := (x_p, x_c, x_l)$  and renewable power generation  $\xi := (\xi_t, \forall t)$  are regarded as parameters, and the decision variables are  $\dot{p}_t^{rs}$ ,  $\dot{p}_t^{rg}$ ,  $\dot{p}_t^{sg}$ ,  $\dot{p}_t^c$ , and  $e_t$ ,  $\forall t$ . Therefore, the optimal value of problem (1), the renewable energy curtailment, can be viewed as a function of  $x$  and  $\xi$ , which is denoted by  $f(x, \xi)$ .

## 2.2 | Ambiguity set

The renewable energy generation  $\xi$  is uncertain. It consists of  $T$  random numbers in  $[0, P_r]$ , where  $P_r$  is the capacity of the renewable power plant. Let  $\Xi = \{\xi \in \mathbb{R}^T | 0 \leq \xi \leq P_r\}$  be the support set of  $\xi$  and  $\mathcal{M}(\Xi)$  the set of distributions  $\mathbb{P}$  supported on  $\Xi$  such that  $\mathbb{E}_{\mathbb{P}}[\|\xi\|_1] < \infty$ , where  $\|\cdot\|_1$  is the 1-norm, and  $\mathbb{E}_{\mathbb{P}}[\cdot]$  is the expectation under distribution  $\mathbb{P}$ .

Assume the real distribution of  $\xi$  is  $\mathbb{P}_0$ .  $\mathbb{P}_0$  is hard to obtain but we can approximate with limited data available at hand. Suppose there are  $N$  samples of  $\xi$  based on the historical weather data, namely  $\xi_n := (\xi_{n,t}, \forall t)$ ,  $n = 1, 2, \dots, N$ . The empirical probability distribution of  $\xi$  is

$$\mathbb{P}_c := \frac{1}{N} \sum_n \mathbf{1}_{\xi_n} \quad (2)$$

where  $\mathbf{1}_{\xi_n}$  denotes the distribution where  $\xi_n$  has probability 1, so for  $\mathbb{P}_c$  each sample is endowed with probability  $1/N$ .

In general,  $\mathbb{P}_c \neq \mathbb{P}_0$ , but  $\mathbb{P}_0$  is typically around  $\mathbb{P}_c$ . Therefore, the ambiguity set considers all possible probability distributions near  $\mathbb{P}_c$ . The distance between two probability distributions is measured by the 1-norm Wasserstein metric [43]

$$d_W(\mathbb{P}_1, \mathbb{P}_2) := \inf_{\Xi \times \Xi} \int \|\xi_1 - \xi_2\|_1 \Pi(d\xi_1, d\xi_2) \quad (3)$$

$\Pi$  is a joint distribution with marginals  $\mathbb{P}_1$  and  $\mathbb{P}_2$

The above definition accounts for both discrete and continuous distributions. With this definition of distance, the ambiguity set is

$$\mathcal{B}(\varepsilon) := \{\mathbb{P} \in \mathcal{M}(\Xi) | d_W(\mathbb{P}, \mathbb{P}_c) \leq \varepsilon\} \quad (4)$$

The ambiguity set  $\mathcal{B}(\varepsilon)$  is comprised of all probability distributions  $\mathbb{P}$  in  $\mathcal{M}(\Xi)$  whose distance to  $\mathbb{P}_c$  is no larger than  $\varepsilon$ , where  $\varepsilon$  is a parameter controlling the radius of the ambiguity set.

*Remark.* The choice of ambiguity sets by decision-makers can be generally categorised into distance-based, moment-based, and shape-preserving ambiguity sets [44]. The moment-based ambiguity set contains the probability distributions whose moments are in the specified range [45]. However, the moment information has its limitation and may not be strong enough to characterise the distribution. Two different distributions may have the same first- and second-order moments. On the contrary, the Wasserstein metric between any two different probability distributions is larger than 0, so it can distinguish probability distributions well [43]. In shape-preserving models, the distributions in the ambiguity set have similar structural properties such as symmetry, unimodality, and convexity, and sometimes the model is incorporated into a moment-based ambiguity set [46]. This method uses more information than the typical moment-based approach but still cannot distinguish all probability distributions. More importantly, there is no concrete knowledge about the aforementioned structural properties of the random multi-period renewable generation as far as we know. Therefore, we choose distance-based ambiguity sets because of their advantages over other types of ambiguity sets for the considered problem.

## 2.3 | Worst-case CVaR constraint of curtailment

Denote by  $\lambda$  the acceptable renewable energy curtailment rate. Then the event of renewable curtailment being acceptable is represented by the formula  $f(x, \xi) \leq \lambda \sum_t \xi_t \Delta_t$ . It is a random event due to the uncertain renewable generation  $\xi$ . A commonly adopted criterion is the event probability, which leads to a robust chance constraint

$$\inf_{\mathbb{P} \in \mathcal{B}(\varepsilon)} \mathbb{P}[f(x, \xi) \leq \lambda \sum_t \xi_t \Delta_t] \geq \beta \quad (5)$$



where  $\beta$  is the minimal acceptable probability;  $\mathbb{P}[\cdot]$  represents the probability of the event in the bracket under distribution  $\mathbb{P}$ . Then constraint (5) means that the probability of acceptable curtailment is always no smaller than  $\beta$  for all the distributions in  $\mathcal{B}(\epsilon)$ , including the worst-case distribution.

Constraint (5) can be viewed as a worst-case risk constraint. In fact, utilising a loss function and the notion of VaR, constraint (5) is equivalent to a worst-case VaR constraint. The loss function is defined by

$$g(x, \xi) = f(x, \xi) - \lambda \sum_t \xi_t \Delta_t \quad (6)$$

which is the difference between the renewable curtailment of optimal operation and the acceptable energy curtailment. Since  $g(x, \xi) \leq 0$  exactly means  $f(x, \xi) \leq \lambda \sum_t \xi_t \Delta_t$ , constraint (5) is equivalent to

$$\inf_{\mathbb{P} \in \mathcal{B}(\epsilon)} \mathbb{P}[g(x, \xi) \leq 0] \geq \beta \quad (7)$$

The  $\beta$ -VaR of the loss function  $g(x, \xi)$  under distribution  $\mathbb{P}$  is defined as

$$\beta\text{-VaR}(x, \mathbb{P}, g) = \min\{y \in \mathbb{R} | \mathbb{P}[g(x, \xi) \leq y] \geq \beta\} \quad (8)$$

which is the smallest threshold  $y$  such that  $g(x, \xi) \leq y$  holds for probability at least  $\beta$ . Therefore,  $\mathbb{P}[g(x, \xi) \leq 0] \geq \beta$  is equivalent to  $\beta\text{-VaR}(x, \mathbb{P}, g) \leq 0$ . Then constraint (7) interprets that for any distribution  $\mathbb{P} \in \mathcal{B}(\epsilon)$ ,  $\beta\text{-VaR}(x, \mathbb{P}, g) \leq 0$ , so Equation (7) is equivalent to

$$\sup_{\mathbb{P} \in \mathcal{B}(\epsilon)} \beta\text{-VaR}(x, \mathbb{P}, g) \leq 0 \quad (9)$$

However, VaR leads to nonconvex constraints. CVaR is a conservative approximation of VaR and is convex [47]. The  $\beta$ -CVaR is defined as

$$\beta\text{-CVaR}(x, \mathbb{P}, g) = \mathbb{E}_{\mathbb{P}}[g(x, \xi) | g(x, \xi) \geq \beta\text{-VaR}(x, \mathbb{P}, g)] \quad (10)$$

which is the conditional expectation of  $g(x, \xi)$  under the condition  $g(x, \xi) \geq \beta\text{-VaR}(x, \mathbb{P}, g)$ . Thus

$$\beta\text{-CVaR}(x, \mathbb{P}, g) \geq \beta\text{-VaR}(x, \mathbb{P}, g)$$

always holds. The worst-case CVaR constraint of curtailment is

$$\sup_{\mathbb{P} \in \mathcal{B}(\epsilon)} \beta\text{-CVaR}(x, \mathbb{P}, g) \leq 0 \quad (11)$$

and according to the analysis above, constraint (11) is a sufficient condition of Equation (5).

*Remark.* We choose CVaR as the risk measure in the proposed method due to the following three reasons. First, CVaR is a risk measure with good properties. It reflects the tail of the distribution and provides information about the expected loss of bad cases. It is coherent, transition-equivariant, positively homoge-

neous, convex, and has some monotonic properties, which help CVaR to become a popular risk measure in finance, engineering, and many other fields [47]. It is also in line with our desire to measure the curtailment risk. Second, CVaR can be equivalently modelled by linear constraints in optimisation problems, which makes it tractable [47]. Based on this advantage of CVaR, we develop the linear programming solution strategy for the proposed sizing model, as Section 3 shows. Third, CVaR is closely related to VaR by the fact that CVaR is the best conservative convex approximation of VaR [48]. The constraint of VaR is equivalent to chance constraint, but VaR is not convex and difficult to deal with. CVaR constraint provides a conservative model of chance constraint, while it avoids the difficulties.

## 2.4 | Sizing problem

The coordinate capacity sizing problem of ESS and transmission line for a remote renewable power plant is formulated as

$$\min_x C_p x_p + C_e x_e + C_l x_l \quad (12a)$$

$$\text{s.t. } x = (x_p, x_e, x_l) \geq 0 \quad (12b)$$

$$\sup_{\mathbb{P} \in \mathcal{B}(\epsilon)} \beta\text{-CVaR}(x, \mathbb{P}, g) \leq 0 \quad (12c)$$

where the objective (12a) is to minimise the total investment cost of the ESS and transmission line; Equation (12b) is the non-negativity constraint of capacities; Equation (12c) is the curtailment constraint.

The sizing model (12) is a DRO problem with a worst-case CVaR constraint based on the Wasserstein-metric ambiguity set. Another dimension of difficulty arises from the definition of loss function  $g(x, \xi)$ ; it involves the optimal value function  $f(x, \xi)$  of linear program (1), whose analytical expression is not available. The above difficulties prevent problem (12) from being solved directly.

## 3 | SOLUTION STRATEGY

In this section, the analytical expression of the curtailment function  $f(x, \xi)$  is analysed by parametric linear programming, an algorithm is developed to produce an approximation, and then the sizing problem (12) is transformed into a linear program that can be efficiently processed by commercial solvers.

### 3.1 | Analytical expression of the curtailment function

For conciseness, write the linear program (1) in a compact form

$$\begin{aligned} f(\theta) &= \min_y c^T y \\ \text{s.t. } A_1 y &\leq b_1 + B_1 \theta, A_2 y = b_2 + B_2 \theta \end{aligned} \quad (13)$$

where  $\theta = (x, \xi)$  is the parameter vector;  $y$  is the vector of decision variables including  $p_i^{rs}, p_i^{rg}, p_i^{sg}, p_i^c$  and  $e_i, \forall i; A_1, A_2, b_1, b_2, B_1, B_2$ , and  $c$  are coefficient matrices or vectors. Problem (13) is a multiparametric linear program with parameter in the constraint right-hand side [49].

Use  $\Theta$  to represent the domain of  $\theta$ , and in the sizing problem

$$\Theta = \{(x, \xi) | x_p \in [0, \bar{x}_p], x_c \in [0, \bar{x}_c], x_l \in [0, \bar{x}_l], \xi \in \Xi\} \quad (14)$$

where  $\bar{x}_p, \bar{x}_c$ , and  $\bar{x}_l$  are upper bounds of  $x_p, x_c$ , and  $x_l$ , respectively. In the following, we derive the analytical expression of function  $f(\theta), \theta \in \Theta$ .

The dual problem of linear program (13) is

$$\begin{aligned} \max_{\gamma, \mu} & (b_1 + B_1\theta)^T \gamma + (b_2 + B_2\theta)^T \mu \\ \text{s.t.} & A_1^T \gamma + A_2^T \mu = c, \gamma \leq 0 \end{aligned} \quad (15)$$

As Equation (13) must have a finite optimal value for  $\theta \in \Theta$  according to the physical meaning of curtailment, by the dual theory of linear programming [50], Equation (15) has the same optimal value as Equation (13). Therefore

$$\begin{aligned} f(\theta) = \max_{\gamma, \mu} & (b_1 + B_1\theta)^T \gamma + (b_2 + B_2\theta)^T \mu \\ \text{s.t.} & (\gamma, \mu) \in \Gamma \end{aligned}$$

where the dual feasible set

$$\Gamma = \{(\gamma, \mu) | A_1^T \gamma + A_2^T \mu = c, \gamma \leq 0\}$$

is a polyhedron. The maximum is achieved at some vertex of  $\Gamma$  because  $f(\theta)$  has finite value. Denote the vertex set of  $\Gamma$  by  $V(\Gamma) = \{(\gamma_k, \mu_k), k = 1, \dots, K\}$ , then

$$\begin{aligned} f(\theta) &= \max_{(\gamma_k, \mu_k) \in V(\Gamma)} (b_1 + B_1\theta)^T \gamma_k + (b_2 + B_2\theta)^T \mu_k \\ &= \max_{(\gamma_k, \mu_k) \in V(\Gamma)} (\gamma_k^T B_1 + \mu_k^T B_2) \theta + (\gamma_k^T b_1 + \mu_k^T b_2) \\ &= \max_{(\gamma_k, \mu_k) \in V(\Gamma)} f_k(\theta) \end{aligned} \quad (16)$$

where

$$f_k(\theta) := (\gamma_k^T B_1 + \mu_k^T B_2) \theta + (\gamma_k^T b_1 + \mu_k^T b_2)$$

is an affine function in  $\theta$ . (16) means that  $f(\theta)$  is the pointwise maximum of finitely many affine functions. Thus,  $f(\theta)$  is convex and piecewise affine.

The number of constraints in Equation (1) determines the dimension of dual variable  $(\gamma, \mu)$ . Because of the operation in multiple periods, the dimension of  $(\gamma, \mu)$  is inevitably high, which leads to enormous vertices of  $\Gamma$ . Therefore, it is not prac-

tical to enumerate all the elements in  $V(\Gamma)$ . Nevertheless, only a small fraction of vertices is necessary to generate the piecewise affine formulation in Equation (16).

### 3.2 | Approximation error

For any subset  $W \subset V(\Gamma)$ ,

$$f(\theta) \geq f_W(\theta) := \max_{(\gamma_k, \mu_k) \in W} f_k(\theta) \quad (17)$$

where  $f_W(\theta)$  is an approximation of  $f(\theta)$  and larger  $W$  incurs more accurate approximation. Because  $f_W(\theta)$  is piecewise affine, it is more convenient to analyse it in the region where it is affine. Clearly, such a region consists of points where a particular piece reaches maximum among all the pieces, that is

$$\Theta_{W,k} = \{\theta | \theta \in \Theta, f_k(\theta) \geq f_l(\theta), \forall (\gamma_l, \mu_l) \in W, l \neq k\} \quad (18)$$

When  $\theta \in \Theta_{W,k}$ , the  $k$ th piece achieves maximum, and  $f_W(\theta) = f_k(\theta)$ . As  $f_k(\theta)$  and  $f_l(\theta)$  are affine functions,  $\Theta_{W,k}$  is a polyhedron. If we use  $f_W(\theta)$  to approximate  $f(\theta)$ , the maximum error in  $\Theta_{W,k}$  can be calculated by

$$\begin{aligned} \max_{\theta \in \Theta_{W,k}} & f(\theta) - f_k(\theta) \\ &= \begin{cases} \max_{\theta, \gamma, \mu} v(\theta, \gamma, \mu) \\ \text{s.t. } \theta \in \Theta_{W,k}, (\gamma, \mu) \in \Gamma \end{cases} \end{aligned} \quad (19)$$

where

$$\begin{aligned} v(\theta, \gamma, \mu) &:= (b_1 + B_1\theta)^T \gamma + (b_2 + B_2\theta)^T \mu \\ &\quad - (\gamma_k^T B_1 + \mu_k^T B_2) \theta - (\gamma_k^T b_1 + \mu_k^T b_2) \end{aligned} \quad (20)$$

by the dual problem (15). Although the feasible region of Equation (19) is polyhedral, the objective is a bilinear function  $v(\theta, \gamma, \mu)$  containing product terms  $\theta^T B_1^T \gamma$  and  $\theta^T B_2^T \mu$ . We adopt the mountain climbing procedure [51] to solve problem (19). It alternatively optimises  $\theta$  and  $(\gamma, \mu)$  with the other variables fixed, so the problems need to be solved are linear programs, as shown in Algorithm 1.

The initial feasible point  $\theta^{(0)} \in \Theta_{W,k}$  is found by computing the Chebyshev centre of  $\Theta_{W,k}$ , which is the centre of the largest ball inside the polyhedron [50]. Transform (18) into the form  $\Theta_{W,k} = \{\theta | u_i^T \theta \leq w_i, \forall i\}$ , where  $u_i$  and  $w_i$  are constant vectors. Then the Chebyshev centre can be found by solving a linear program [50]

$$\begin{aligned} \max_{r, \theta} & r \\ \text{s.t.} & u_i^T \theta + r \|u_i\|_2 \leq w_i, \forall i \end{aligned} \quad (22)$$

**ALGORITHM 1** Mountain climbing

**Input:** Data of problem (19), initial feasible point  $\theta^{(0)} \in \Theta_{W,k}$ , and a small positive number  $\delta > 0$  for convergence criterion.

**Output:** A solution  $(\theta^{(i)}, \gamma^{(i)}, \mu^{(i)})$  of problem (19).

- 1: Initiation:  $i \leftarrow 1$ .
- 2: Solve linear program  $\max_{(\gamma, \mu) \in \Gamma} v(\theta^{(i-1)}, \gamma, \mu)$  and find the optimal solution  $(\gamma^{(i)}, \mu^{(i)})$ .
- 3: Solve linear program  $\max_{\theta \in \Theta_{W,k}} v(\theta, \gamma^{(i)}, \mu^{(i)})$  and find the optimal solution  $\theta^{(i)}$ .
- 4: Terminate if
 
$$v(\theta^{(i)}, \gamma^{(i)}, \mu^{(i)}) - v(\theta^{(i-1)}, \gamma^{(i)}, \mu^{(i)}) \leq \delta \quad (21)$$
 Otherwise, update  $i \leftarrow i + 1$ , and turn to Step 2.

**ALGORITHM 2** Curtailment function approximation

**Input:** Data of problem (13), a set  $\Theta_0$  containing typical values of  $\theta$  for initiation, and a small positive number  $\delta > 0$  for convergence criterion.

**Output:** An approximation  $f_{W'}(\theta)$  for  $f(\theta)$ .

- 1: Initiation:  $W' \leftarrow \emptyset$ . For every  $\theta_k \in \Theta_0$ , solve problem (15) with  $\theta = \theta_k$  and find the optimal solution  $(\gamma_k, \mu_k)$ . If  $(\gamma_k, \mu_k) \notin W'$ , update  $W' \leftarrow W' \cup \{(\gamma_k, \mu_k)\}$ .
- 2:  $W' \leftarrow W'$ . For every  $(\gamma_k, \mu_k) \in W'$ , find  $\Theta_{W',k}$  by Equation (18). Solve problem (22) and obtain  $\theta^{(0)} \in \Theta_{W',k}$ . Use Algorithm 1 with the initial feasible point  $\theta^{(0)}$  to find a solution of problem (19) and obtain  $(\theta^*, \gamma^*, \mu^*)$ . If  $v(\theta^*, \gamma^*, \mu^*) > \delta$ , solve problem (15) with  $\theta = \theta^*$  and find the optimal solution  $(\gamma', \mu')$ . If  $(\gamma', \mu') \notin W'$ , update  $W' \leftarrow W' \cup \{(\gamma', \mu')\}$ .
- 3: If  $W' = W$ , terminate and output  $f_{W'}(\theta)$ . Otherwise, update  $W' \leftarrow W'$  and turn to Step 2.

where  $\|\cdot\|_2$  represents the 2-norm, and the Chebyshev centre is the value of  $\theta$  in the optimal solution.

**3.3 | Approximate the curtailment function**

Combining the above steps, the algorithm to compute the curtailment function is given in Algorithm 2.

The idea of Algorithm 2 is identifying necessary dual vertices by solving a series of linear program. Step 1 and 2 guarantee that  $f_k(\theta_k) = f(\theta_k)$ , so  $\Theta_{W',k}$  is nonempty for any  $(\gamma_k, \mu_k) \in W'$ . In addition, Algorithm 2 always converges because  $V(\Gamma)$  has finite elements.

**3.4 | Transforming the sizing problem into a linear program**

The sizing problem (12) cannot be directly solved because of the worst-case CVaR constraint (12c) or (11). With the help of CVaR properties, Equation (11) will be transformed into a worst-case expectation constraint, and it leads to a linear pro-

gram thanks to the curtailment function expression (17) provided by Algorithm 2.

According to Theorem 1 in ref. [47],  $\beta$ -CVaR can be determined from

$$\beta\text{-CVaR}(x, \mathbb{P}, g) = \inf_{\alpha \in \mathbb{R}} \left\{ \alpha + \frac{1}{1-\beta} \mathbb{E}_{\mathbb{P}}[\max\{g(x, \xi) - \alpha, 0\}] \right\} \quad (23)$$

Additionally by the stochastic saddle point theorem [52],  $\sup_{\mathbb{P} \in B(\varepsilon)}$  and  $\inf_{\alpha \in \mathbb{R}}$  can be swapped, i.e.

$$\begin{aligned} & \sup_{\mathbb{P} \in B(\varepsilon)} \beta\text{-CVaR}(x, \mathbb{P}, g) \\ &= \sup_{\mathbb{P} \in B(\varepsilon)} \inf_{\alpha \in \mathbb{R}} \left\{ \alpha + \frac{1}{1-\beta} \mathbb{E}_{\mathbb{P}}[\max\{g(x, \xi) - \alpha, 0\}] \right\} \\ &= \inf_{\alpha \in \mathbb{R}} \sup_{\mathbb{P} \in B(\varepsilon)} \left\{ \alpha + \frac{1}{1-\beta} \mathbb{E}_{\mathbb{P}}[\max\{g(x, \xi) - \alpha, 0\}] \right\} \\ &= \inf_{\alpha \in \mathbb{R}} \left\{ \alpha + \frac{1}{1-\beta} \sup_{\mathbb{P} \in B(\varepsilon)} \mathbb{E}_{\mathbb{P}}[\max\{g(x, \xi) - \alpha, 0\}] \right\} \end{aligned} \quad (24)$$

Hence, the constraint (11) is equivalently transformed into the following constraint about worst-case expectation.

$$\alpha + \frac{1}{1-\beta} \sup_{\mathbb{P} \in B(\varepsilon)} \mathbb{E}_{\mathbb{P}}[\max\{g(x, \xi) - \alpha, 0\}] \leq 0 \quad (25)$$

By Algorithm 2,  $f(x, \xi)$  is approximated by the maximum of some affine functions, hence  $g(x, \xi) = f(x, \xi) - \lambda \sum_t \xi_t \Delta_t$  has the same form, i.e.

$$g(x, \xi) = \max_k d_{1,k}^T x + d_{2,k}^T \xi + d_{3,k} \quad (26)$$

for some constant coefficients  $d_{1,k}$ ,  $d_{2,k}$  and  $d_{3,k}$ . Then

$$\begin{aligned} & \max\{g(x, \xi) - \alpha, 0\} \\ &= \max_k \{ \max_{\xi} d_{2,k}^T \xi + (d_{1,k}^T x + d_{3,k} - \alpha), 0 \} \end{aligned} \quad (27)$$

is the maximum of some affine functions.

Write  $\Xi$  into the form  $\Xi = \{\xi \in \mathbb{R}^T | H\xi \leq b\}$  for constant matrix  $H$  and vector  $b$ . Then according to Corollary 5.1 in ref. [43], the worst-case expectation  $\sup_{\mathbb{P} \in B(\varepsilon)} \mathbb{E}_{\mathbb{P}}[\max\{g(x, \xi) - \alpha, 0\}]$  evaluates to

$$\inf_{\rho, \sigma} \varepsilon \rho + \frac{1}{N} \sum_n s_n \quad (28a)$$

$$\text{s.t. } \sigma_{nk} \geq 0, \forall n, k, \sigma_{n0} \geq 0, \forall n \quad (28b)$$



$$d_{1,k}^T x + d_{3,k} - \alpha + d_{2,k}^T \xi_n + (b - H\xi_n)^T \sigma_{nk} \leq s_n, \forall n, k \quad (28c)$$

$$(b - H\xi_n)^T \sigma_{n0} \leq s_n, \forall n \quad (28d)$$

$$\|H^T \sigma_{nk} - d_{2,k}\|_\infty \leq \rho, \forall n, k \quad (28e)$$

$$\|H^T \sigma_{n0}\|_\infty \leq \rho, \forall n \quad (28f)$$

where  $\|\cdot\|_\infty$  is the  $\infty$ -norm.

By its definition,  $\|H^T \sigma_{nk} - d_{2,k}\|_\infty \leq \rho$  is equivalent to the joint inequality consisting of  $H^T \sigma_{nk} - d_{2,k} \leq \rho 1_T$  and  $-H^T \sigma_{nk} + d_{2,k} \leq \rho 1_T$ , where  $1_T$  is the  $T$ -dimensional vector of ones.  $\|H^T \sigma_{n0}\|_\infty$  can be handled similarly. Combine them with Equation (25), then the linear program formulation of the capacity sizing problem (12) is as follows

$$\begin{aligned} \min_{x, \alpha, \rho, s, \sigma} \quad & C_p x_p + C_e x_e + C_l x_l \\ \text{s.t.} \quad & x_p, x_e, x_l \geq 0 \\ & \alpha + \frac{1}{1-\beta} \left( \varepsilon \rho + \frac{1}{N} \sum_n s_n \right) \leq 0 \\ & H^T \sigma_{nk} - d_{2,k} \leq \rho 1_T, \forall n, k \\ & -H^T \sigma_{nk} + d_{2,k} \leq \rho 1_T, \forall n, k \\ & H^T \sigma_{n0} \leq \rho 1_T, -H^T \sigma_{n0} \leq \rho 1_T, \forall n \\ & (28b), (28c), (28d) \end{aligned} \quad (29)$$

Linear program (29) is an approximation of the sizing problem (12). The optimal sizing strategy offered by Equation (29) guarantees the probability of curtailment rate being higher than the threshold less than  $1 - \beta$  even in the worst-case distribution of renewable generation.

## 4 | CASE STUDY

### 4.1 | System configurations

A remote PV power plant with an installed capacity of 1 GW is used to validate the proposed method. The hourly solar radiation data of one year are obtained from the National Solar Radiation Database [53], based on which the hourly power generation is simulated, and shown in Figure 2. Among them 120 days of data are selected for planning by choosing 10 days in each month. The remaining 245 days make up the test data. In the benchmark case,  $T = 24$ ,  $N = 120$ ,  $\Delta_t = 1$  h,  $P_r = 1$  GW, and  $\xi_{n,t}$  are from the 120 days of data for planning. The parameters of ESS are  $\eta_c = \eta_d = 0.95$ ,  $\omega_l = 0.1$ ,  $\omega_h = 0.9$ ,  $C_p = 10^6$  ¥/MW, and  $C_e = 1.2 \times 10^6$  ¥/MWh. The parameter of transmission line is  $C_l = 2 \times 10^7$  ¥/MW. Other parameters

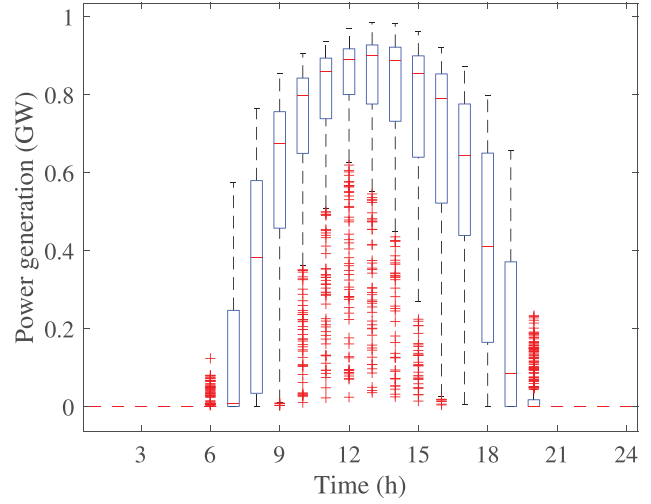


FIGURE 2 Boxplot of the hourly power generation

are  $\varepsilon = 0.005$ ,  $\lambda = 5\%$ , and  $\beta = 0.9$ . The proposed method is coded in MATLAB using YALMIP toolbox [54]; optimisation problems are solved by Gurobi 9.1 [55].

### 4.2 | Curtailment function

The first step of the proposed method is to find the approximate expression of the curtailment function, in which the independent variables are renewable generation  $\xi = (\xi_t, \forall t)$  and capacity variable  $x = (x_p, x_e, x_l)$ . Since the capacity of PV power generation is 1 GW, the range  $\Theta$  of independent variables is set by  $0 \leq \xi_t \leq 1$  GW,  $\forall t$ ,  $0 \leq x_p \leq 1$  GW,  $0 \leq x_e \leq 12$  GWh, and  $0 \leq x_l \leq 1$  GW. As for the initiation in Algorithm 2, the 120 days of renewable generation data are used for  $\xi$ , and  $x$  is initiated by randomly generated values with mean  $x_p = 0.85$  GW,  $x_e = 5.4$  GWh, and  $x_l = 0.39$  GW. Specifically, evenly generate a value between 0.85–1.15 and multiply it to the mean value.  $x_p$ ,  $x_e$ , and  $x_l$  are generated separately and independently. These mean values are chosen according to the results of the traditional optimisation methods explained later.

The 120 initial values of  $\theta$  result in 19 distinct vertices in  $V(\Gamma)$ . After six iterations in Algorithm 2 and totally 248s for computation, we obtain a subset  $W$  of  $V(\Gamma)$  consisting of 46 vertices and the approximate expression  $f_W(x, \xi)$  which is the maximum of 46 affine functions.

In order to test the accuracy of  $f_W(x, \xi)$ , use the 245 days of renewable generation testing data, and newly generated 245 typical capacity values. Compare the estimated curtailment values provided by  $f_W(x, \xi)$  and the exact curtailment calculated by solving the operation problem (1). The results are depicted in Figure 3, which shows that the approximate values are near the correct results in almost all cases.

The curtailment function has 27 independent variables. By fixing the value of  $\xi$  at a typical day, the curtailment function is visualised in Figure 4. In Figure 4(a),  $x_l$  is fixed at 0.39 GW; in Figure 4(b),  $x_e/x_p = 6$  h. The curtailment decreases as  $x_p$ ,  $x_e$ , or  $x_l$  increases.

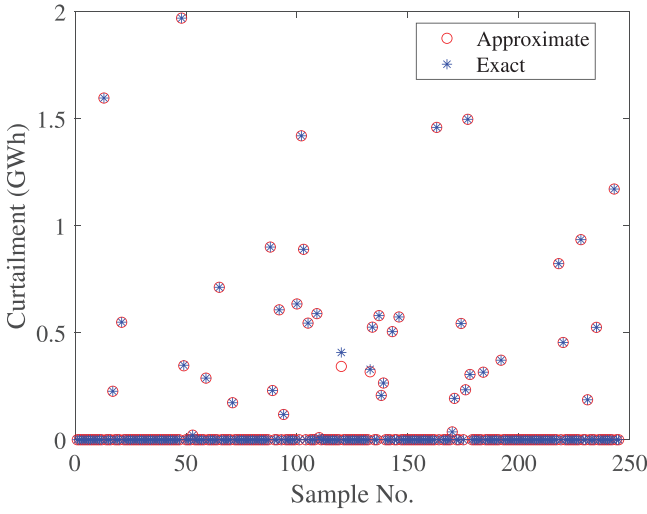


FIGURE 3 Accuracy of the curtailment function approximation

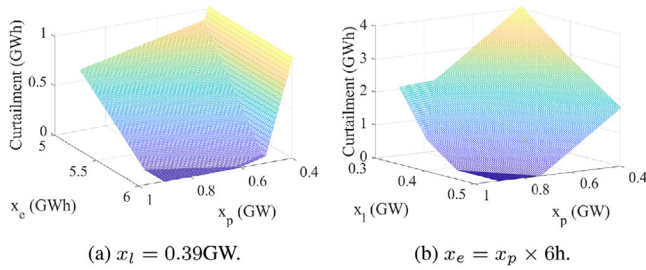


FIGURE 4 Visualisations of the curtailment function

### 4.3 | Other sizing models for comparison

Four cases are considered for comparison

- Case 1 (benchmark case): The proposed method.
- Case 2: Stochastic optimisation based on CVaR.
- Case 3: Robust optimisation.
- Case 4: DRO with a Wasserstein-metric ambiguity set considering only discrete distributions supported on  $\{\xi_n, \forall n\}$ .

The stochastic optimisation model assumes  $\mathbb{P}_0 = \mathbb{P}_e$  and neglects the inexactness of empirical distribution. The curtailment constraint (12c) in the sizing problem is substituted by  $\beta$ -CVaR( $x, \mathbb{P}_e, g$ )  $\leq 0$ , which means that the CVaR of curtailment is evaluated with respect to  $\mathbb{P}_e$ . Utilising Equation (23), the model is equivalent to the following linear program.

$$\begin{aligned}
 & \min C_p x_p + C_e x_e + C_l x_l \\
 & \text{s.t. } x_p, x_e, x_l \geq 0, \alpha + \frac{1}{N(1-\beta)} \sum_n s_n \leq 0 \\
 & s_n \geq \sum_t \hat{p}_{n,t}^c \Delta_t - \lambda \sum_t \xi_{n,t} \Delta_t - \alpha, s_n \geq 0, \forall n \\
 & (1b) - (1b), \forall n
 \end{aligned} \quad (30)$$

In the robust optimisation model, the curtailment rate is required to be no larger than  $\lambda$  for any data sample, i.e.  $g(x, \xi_n) \leq 0, \forall n$ , so the equivalent linear program is

$$\begin{aligned}
 & \min C_p x_p + C_e x_e + C_l x_l \\
 & \text{s.t. } x_p, x_e, x_l \geq 0 \\
 & \sum_t \hat{p}_{n,t}^c \Delta_t - \lambda \sum_t \xi_{n,t} \Delta_t \leq 0, \forall n \\
 & (1b) - (1b), \forall n
 \end{aligned} \quad (31)$$

In the DRO model considering only discrete distributions supported on  $\{\xi_n, \forall n\}$ , each distribution can be represented by a vector  $q = (q_n, \forall n)$  in which  $q_n$  is the probability of  $\xi_n$ . Then the ambiguity set is

$$\mathcal{B}_d(\epsilon) = \left\{ \mathbb{P} = \sum_n q_n \mathbf{1}_{\xi_n} \mid \begin{aligned} & q_n \geq 0, \forall n \\ & \sum_n q_n = 1 \\ & d_W(\mathbb{P}, \mathbb{P}_e) \leq \epsilon \end{aligned} \right\} \quad (32)$$

According to the definitions of  $\mathcal{B}_d(\epsilon)$  and Wasserstein metric in Equations (32) and (3), respectively, the worst-case expectation in Equation (25) with ambiguity set  $\mathcal{B}_d(\epsilon)$  evaluates to

$$\begin{aligned}
 & \sup_{\mathbb{P} \in \mathcal{B}_d(\epsilon)} \mathbb{E}_{\mathbb{P}} [\max\{g(x, \xi) - \alpha, 0\}] \\
 & = \begin{cases} \sup_{q, K} \sum_n q_n [\max\{g(x, \xi_n) - \alpha, 0\}] \\ \text{s.t. } \sum_{m,n} K_{mn} \|\xi_m - \xi_n\|_1 \leq \epsilon, \sum_m q_m = 1 \\ K_{mn} \geq 0, \forall m, n \\ \sum_m K_{mn} = 1/N, \forall n \\ \sum_n K_{mn} = q_m, q_m \geq 0, \forall m \end{cases} \\
 & = \begin{cases} \min_{\rho, \nu, \sigma, \tau} \epsilon \rho + \sum_n \frac{\sigma_n}{N} + \tau \\ \text{s.t. } \rho \|\xi_m - \xi_n\|_1 + \nu_m + \sigma_n \geq 0, \forall m, \forall n \\ \rho \geq 0, -\nu_n + \tau \geq \max\{g(x, \xi_n) - \alpha, 0\}, \forall n \end{cases}
 \end{aligned} \quad (33)$$

where the second equality follows from the strong duality of linear programming [50].

Therefore, the sizing model in Case 4 is equivalent to the following linear program.

$$\begin{aligned}
 & \min C_p x_p + C_e x_e + C_l x_l \\
 & \text{s.t. } x_p, x_e, x_l \geq 0
 \end{aligned}$$

**TABLE 1** Results comparison of different methods

| Case | $x_p$<br>[GW] | $x_e$<br>[GWh] | $x_l$<br>[GW] | Cost<br>( $10^9$ ¥) | Test CVaR | Time<br>[s] |
|------|---------------|----------------|---------------|---------------------|-----------|-------------|
| 1    | 0.8508        | 5.4617         | 0.3956        | 15.3175             | -0.0074   | 25          |
| 2    | 0.8487        | 5.3783         | 0.3935        | 15.1722             | 0.0327    | 3           |
| 3    | 0.8878        | 5.5408         | 0.3982        | 15.5002             | -0.0493   | 3           |
| 4    | 0.8834        | 5.4336         | 0.3937        | 15.2777             | 0.0050    | 5           |

$$\begin{aligned}
& \alpha + \frac{1}{1-\beta} \left( \varepsilon \rho + \sum_n \frac{\sigma_n}{N} + \tau \right) \leq 0, \rho \geq 0 \\
& \rho \|\xi_m - \xi_n\|_1 + \nu_m + \sigma_n \geq 0, \forall m, \forall n \\
& -\nu_n + \tau \geq \sum_t \hat{p}_{n,t}^c \Delta_t - \lambda \sum_t \xi_{n,t} \Delta_t - \alpha, \forall n \\
& -\nu_n + \tau \geq 0, (1b) - (1b), \forall n
\end{aligned} \quad (34)$$

#### 4.4 | Sizing results and comparison

The sizing results of all the cases are compared in Table 1. To test the conservative degree, the  $\beta$ -CVaR of loss function  $g$  is calculated utilising the 245 days of data according to the formula in Equation (23).

As the results show in Table 1, the test CVaR is smaller than 0 in the benchmark case, validating the effectiveness of the proposed method. In Case 2, the inexactness of the empirical distribution is not considered, so the result is optimistic, reflected by the positive test CVaR. The result of Case 3 has the highest cost and lowest CVaR, due to the conservativeness of robust optimisation. However, this result still causes unacceptable curtailment scenarios in the test data, since the empirical distribution does not cover all the extreme situations. In fact, if the robust optimisation method is applied to the total 365 days of data, then the investment cost reaches  $15.9769 \times 10^9$  ¥, which is much higher. The result of Case 4 is more conservative than Case 2 but more optimistic than Case 3. This is because  $\mathbb{P}_e \in \mathcal{B}_d(\varepsilon) \subset \mathcal{B}(\varepsilon)$  by the definitions of ambiguity sets in Equations (4) and (32). The results of Case 1 and Case 4 are different, which means  $\mathcal{B}_d(\varepsilon) \subsetneq \mathcal{B}(\varepsilon)$  and the worst-case distribution of  $\mathcal{B}(\varepsilon)$  is not contained in  $\mathcal{B}_d(\varepsilon)$ . Therefore, the DRO method used in Case 4 has its limitation since the worst-case distribution is not captured by Equation (32).

The computation times of solving the four capacity sizing models are shown in the last column of Table 1. The efficiency is sufficiently high for a planning problem.

#### 4.5 | Parameter sensitivity analysis

The impacts of some parameters are investigated, including the ambiguity set radius  $\varepsilon$ , the data amount  $N$ , the acceptable probability  $\beta$ , the acceptable curtailment rate  $\lambda$ , and the unit capacity cost  $C_l$  of transmission line.

**TABLE 2** Results under different  $\varepsilon$ 

| $\varepsilon$ | $x_p$<br>[GW] | $x_e$<br>[GWh] | $x_l$<br>[GW] | Cost<br>( $10^9$ ¥) | Test CVaR | Time<br>[s] |
|---------------|---------------|----------------|---------------|---------------------|-----------|-------------|
| 0.000         | 0.8487        | 5.3783         | 0.3935        | 15.1722             | 0.0327    | 24          |
| 0.001         | 0.8493        | 5.3876         | 0.3941        | 15.1970             | 0.0241    | 24          |
| 0.002         | 0.8494        | 5.4092         | 0.3942        | 15.2249             | 0.0169    | 24          |
| 0.005         | 0.8508        | 5.4617         | 0.3956        | 15.3175             | -0.0074   | 25          |
| 0.010         | 0.8901        | 5.5309         | 0.4004        | 15.5355             | -0.0622   | 24          |

**TABLE 3** Results under different  $N$ 

| $N$ | $x_p$<br>[GW] | $x_e$<br>[GWh] | $x_l$<br>[GW] | Cost<br>( $10^9$ ¥) | Test CVaR | Time<br>[s] |
|-----|---------------|----------------|---------------|---------------------|-----------|-------------|
| 48  | 0.8351        | 5.4058         | 0.3946        | 15.2143             | 0.0192    | 5           |
| 72  | 0.8348        | 5.3906         | 0.3943        | 15.1901             | 0.0264    | 7           |
| 96  | 0.8506        | 5.4580         | 0.3954        | 15.3077             | -0.0048   | 15          |
| 120 | 0.8508        | 5.4617         | 0.3956        | 15.3175             | -0.0074   | 25          |

**TABLE 4** Results under different  $\lambda$ 

| $\lambda$ | $x_p$<br>[GW] | $x_e$<br>[GWh] | $x_l$<br>[GW] | Cost<br>( $10^9$ ¥) | $\zeta$ | Time<br>[s] |
|-----------|---------------|----------------|---------------|---------------------|---------|-------------|
| 3%        | 0.8959        | 5.6158         | 0.4063        | 15.7606             | 0.0023  | 25          |
| 5%        | 0.8508        | 5.4617         | 0.3956        | 15.3175             | 0.0064  | 25          |
| 7%        | 0.8427        | 5.2923         | 0.3875        | 14.9444             | 0.0125  | 25          |
| 10%       | 0.8290        | 5.0934         | 0.3738        | 14.4169             | 0.0235  | 25          |
| 15%       | 0.7868        | 4.7760         | 0.3519        | 13.5554             | 0.0480  | 25          |

The sizing results under different ambiguity set radius  $\varepsilon$  are presented in Table 2. As  $\varepsilon$  increases, the results become more conservative. The reason is that the ambiguity set gets larger as a Wasserstein-metric ball centred at  $\mathbb{P}_e$ , and worse distributions are included. In the case of  $\varepsilon = 0$ , the ambiguity set degenerates to a single distribution  $\{\mathbb{P}_e\}$ , and the proposed sizing model degenerates to the stochastic programming method in Case 2. Their results coincide, which again verify that the curtailment function is accurate.

Table 3 shows the sizing results under different  $N$ . The computation time increases as  $N$  becomes larger. In general, more data make the empirical distribution  $\mathbb{P}_e$  closer to the real distribution  $\mathbb{P}_0$ . When choosing the radius  $\varepsilon$ , the conservative preference and the data amount  $N$  should be considered together. According to Proposition 3 in ref. [56], the probability of  $d_w(\mathbb{P}_e, \mathbb{P}_0) \leq \varepsilon$ , i.e. the event that the ambiguity set contains the real distribution, is no smaller than  $1 - \exp(-N\varepsilon^2/(2\Phi^2))$ , where  $\Phi$  is the diameter of  $\Xi$ , i.e.  $\Phi := \sup\{\|\xi_1 - \xi_2\|_1 | \xi_1, \xi_2 \in \Xi\}$ . Therefore, to guarantee a confidence level,  $\varepsilon$  should be proportional to  $\sqrt{1/N}$  and  $\Phi$ .

The impacts of the acceptable curtailment rate  $\lambda$  are shown in Table 4. Since the definitions of loss function  $g$  and CVaR

**TABLE 5** Results under different  $\beta$ 

| $\beta$ | $x_p$<br>[GW] | $x_e$<br>[GWh] | $x_l$<br>[GW] | Cost<br>( $10^9$ ¥) | $\kappa$ | Time<br>[s] |
|---------|---------------|----------------|---------------|---------------------|----------|-------------|
| 0.80    | 0.4696        | 5.4360         | 0.3975        | 14.9423             | 0.9224   | 25          |
| 0.84    | 0.8265        | 5.3502         | 0.3915        | 15.0774             | 0.9510   | 24          |
| 0.87    | 0.8346        | 5.3872         | 0.3941        | 15.1813             | 0.9592   | 25          |
| 0.90    | 0.8508        | 5.4617         | 0.3956        | 15.3175             | 0.9796   | 25          |
| 0.93    | 0.8902        | 5.5333         | 0.4006        | 15.5420             | 0.9878   | 26          |

**TABLE 6** Results under different  $C_l$ 

| $C_l$<br>( $10^7$ /MW) | $x_p$<br>[GW] | $x_e$<br>[GWh] | $x_l$<br>[GW] | Cost<br>( $10^9$ ¥) | Time<br>[s] |
|------------------------|---------------|----------------|---------------|---------------------|-------------|
| 1.2                    | 0             | 0              | 0.8481        | 10.1771             | 26          |
| 1.4                    | 0.0961        | 1.0273         | 0.7520        | 11.8564             | 26          |
| 1.6                    | 0.1991        | 2.1274         | 0.6579        | 13.2787             | 25          |
| 1.8                    | 0.3741        | 4.3855         | 0.4882        | 14.4236             | 25          |
| 2.0                    | 0.8508        | 5.4617         | 0.3956        | 15.3175             | 25          |

depend on  $\lambda$ , here the average curtailment rate  $\zeta$  in the test data is used to measure the conservative degree. Larger  $\lambda$  represents a lower requirement for curtailment, so the total investment becomes lower and  $\zeta$  becomes larger. Because the planning maintains the acceptable curtailment rate  $\lambda$  with probability at least  $\beta = 0.90$  even under the worst-case distribution, the average curtailment rate  $\zeta$  is much lower than  $\lambda$ .

Table 5 presents the results with varying acceptable probability  $\beta$ . The definition of CVaR also depends on  $\beta$ , so  $\kappa$ , the probability of curtailment rate being acceptable, is chosen to verify the effectiveness. The total investment cost decreases as  $\beta$  decreases, and so does  $\kappa$ . In addition,  $\kappa$  is always larger than  $\beta$ , since the proposed method guarantees  $\beta$  for the worst-case distribution.

The unit capacity cost of the transmission line largely depends on the length of the transmission corridor. The impacts of  $C_l$  are investigated in Table 6. When the transmission line is cheap, the optimal solution is to merely build the transmission line, and in this situation, the required capacity of the transmission line is still lower than 1 GW. When  $C_l \geq 1.4 \times 10^7$  ¥/MW, equipping ESS may help to reduce the total investment cost. In this situation,  $C_l : C_p : C_e = 14 : 1 : 1.2$ . If the transmission line is in the 500 kV voltage level with a unit cost  $3 \times 10^6$  ¥/km, then its length is about 500 km. A larger  $C_l$  leads to a larger ESS capacity, a smaller transmission line capacity, and a larger total investment cost.

## 5 | CONCLUSION

This paper focuses on coordinately sizing ESS and transmission line for a remote renewable power plant. The optimal operation problem is formulated to minimise the renewable energy

curtailment, which is regarded as a function of the capacity parameters and the uncertain renewable generation. The curtailment function is proven to be piecewise affine and can be calculated approximately via solving linear programs. The distributionally robust capacity sizing problem with distributionally robust curtailment constraint can be approximated by a linear program, utilising VaR and CVaR as well as the worst-case expectation under a Wasserstein-metric-based ambiguity set. Some findings in the case study are summarised.

- 1) The worst-case distribution in the Wasserstein-metric ambiguity set is not a discrete distribution.
- 2) The radius of the ambiguity set should be chosen according to data amount and risk preference. A recommended setting is to choose  $\varepsilon$  proportional to  $\sqrt{1/N}$  and the diameter of the support set.
- 3) The unit capacity cost of the transmission line has an important impact on the sizing results. When the transmission line is longer than 500 km, ESS equipment may help to reduce the total investment cost.

The model and method can be extended to consider the power transmission network with linear models since the proposed solution strategy is based on the linear form of the operation problem. Our future research is aimed at the coordinated renewable generation, transmission, and storage sizing in bulk power systems considering distributionally robust risk.

## NOMENCLATURE

### Abbreviations

|      |                                      |
|------|--------------------------------------|
| PV   | Photovoltaic                         |
| ESS  | Energy storage system                |
| SP   | Stochastic programming               |
| RO   | Robust optimisation                  |
| DRO  | Distributionally robust optimisation |
| SoC  | State of charge                      |
| VaR  | Value-at-Risk                        |
| CVaR | Conditional Value-at-Risk            |

### Parameters

|                      |   |
|----------------------|---|
| $T$                  | The number of time periods                      |
| $N$                  | The number of data samples                      |
| $\Delta_t$           | Period length                                   |
| $\xi_{n,t}$          | Renewable power generation                      |
| $\eta_c, \eta_d$     | Charging and discharging efficiencies           |
| $\omega_l, \omega_h$ | The lower and upper bounds of SoC               |
| $P_r$                | The capacity of renewable power generation      |
| $\varepsilon$        | The radius of ambiguity set                     |
| $C_p$                | The unit power capacity cost of ESS             |
| $C_e$                | The unit energy capacity cost of ESS            |
| $C_l$                | The unit capacity cost of the transmission line |
| $\lambda$            | Acceptable curtailment rate                     |
| $\beta$              | Acceptable probability                          |



## Variables

|                |  |
|----------------|--|
| $x_p$          | The power capacity of ESS                          |
| $x_e$          | The energy capacity of ESS                         |
| $x_l$          | Power capacity of the transmission line            |
| $p_{n,t}^{rs}$ | Power from the generation to the storage           |
| $p_{n,t}^{rg}$ | Power from the generation to the transmission line |
| $p_{n,t}^{sg}$ | Power from the storage to the transmission line    |
| $p_{n,t}^c$    | Renewable power generation curtailment             |
| $e_{n,t}$      | Stored energy                                      |

## ACKNOWLEDGMENTS

This work was supported by the National Natural Science Foundation of China (51807101, U1766203).

## CONFLICT OF INTEREST

The authors declare no conflict of interest.

## ORCID

Rui Xie  <https://orcid.org/0000-0001-9337-0841>

Ming-Feng Ge  <https://orcid.org/0000-0002-6828-0147>

## REFERENCES

- Bakhtiari, H., Naghizadeh, R.A.: Multi-criteria optimal sizing of hybrid renewable energy systems including wind, photovoltaic, battery, and hydrogen storage with  $\epsilon$ -constraint method. *IET Renew. Power. Gener.* 12(8), 883–892 (2018)
- IEA: Renewables information: Overview. IEA (2021). <https://www.iea.org/reports/renewables-information-overview/supply>. Accessed 20 September 2021
- Yang, L.: Ensure energy stability while adjusting the mix. *China Daily* (2021). <https://www.chinadaily.com.cn/a/202110/08/WS615f7e12a310cdd39bc6d5fc.html>. Accessed 25 November 2021
- NS energy: Bhadla solar park, Rajasthan. NS energy (2018). <https://www.nsenergybusiness.com/projects/bhadla-solar-park-rajasthan/>. Accessed 25 November 2021
- Bellini, E.: World's largest solar plant goes online in China - 2.2GW. *PV magazine* (2020). <https://pv-magazine-usa.com/2020/10/02/worlds-largest-solar-plant-goes-online-in-china/>. Accessed 25 November 2021
- Fairley, P.: China's potent wind potential. *MIT Technology Review* (2009). <https://www.technologyreview.com/2009/09/14/209991/chinas-potent-wind-potential/>. Accessed 25 November 2021
- Nathan, S.: The big project: London array. *The Engineer* (2012). <https://www.theengineer.co.uk/the-big-project-london-array/>. Accessed 25 November 2021
- Gonzalez-Gonzalez, J.M., Martin, S., Lopez, P., Aguado, J.A.: Hybrid battery-ultracapacitor storage system sizing for renewable energy network integration. *IET Renew. Power. Gener.* 13(14), 2367–2375 (2020)
- Tang, Z., Liu, J., Liu, Y., Huang, Y., Jawad, S.: Risk awareness enabled sizing approach for hybrid energy storage system in distribution network. *IET Gener. Transm. Distrib.* 13(17), 3814–3822 (2019)
- Sheibani, M.R., Yousefi, G.R., Latify, M.A., Hacopian, Dolatabadi, S.: Energy storage system expansion planning in power systems: a review. *IET Renew. Power. Gener.* 12(11), 1203–1221 (2018)
- Aguado, J.A., de la Torre, S., Triviño, A.: Battery energy storage systems in transmission network expansion planning. *Electr. Power Syst. Res.* 145, 63–72 (2017)
- Neetzow, P., Pechan, A., Eisenack, K.: Electricity storage and transmission: complements or substitutes? *Energy Econ.* 76, 367–377 (2018)
- Khastieva, D., Hesamzadeh, M.R., Vogelsang, I., Rosellón, J., Amelin, M.: Value of energy storage for transmission investments. *Energy Strategy Rev.* 24, 94–110 (2019)
- Nemati, H., Latify, M.A., Yousefi, G.R.: Optimal coordinated expansion planning of transmission and electrical energy storage systems under physical intentional attacks. *IEEE Syst. J.* 14(1), 793–802 (2020)
- Kazemi, M., Ansari, M.R.: An integrated transmission expansion planning and battery storage systems placement - a security and reliability perspective. *Int. J. Electr. Power Energy Syst.* 134, 107329 (2022)
- Mazaheri, H., Abbaspour, A., Fotuhi.Firuzabad, M., Moeini.Aghaie, M., Farzin, H., Wang, F., et al.: An online method for MILP co-planning model of large-scale transmission expansion planning and energy storage systems considering  $n-1$  criterion. *IET Gener. Transm. Distrib.* 15(4), 664–677 (2021)
- Dvorkin, Y., Fernández-Blanco, R., Wang, Y., Xu, B., Kirschen, D.S., Pandžić, H., et al.: Co-planning of investments in transmission and merchant energy storage. *IEEE Trans. Power Syst.* 33(1), 245–256 (2018)
- Bustos, C., Sauma, E., de la Torre, S., Aguado, J.A., Contreras, J., Pozo, D.: Energy storage and transmission expansion planning: substitutes or complements? *IET Gener. Transm. Distrib.* 12(8), 1738–1746 (2018)
- Gan, W., Ai, X., Fang, J., Yan, M., Yao, W., Zuo, W., et al.: Security constrained co-planning of transmission expansion and energy storage. *Appl. Energy* 239, 383–394 (2019)
- Wu, X., Jiang, Y.: Source-network-storage joint planning considering energy storage systems and wind power integration. *IEEE Access* 7, 137330–137343 (2019)
- Zhang, C., Cheng, H., Liu, L., Zhang, H., Zhang, X., Li, G.: Coordination planning of wind farm, energy storage and transmission network with high-penetration renewable energy. *Int. J. Electr. Power Energy Syst.* 120, 105944 (2020)
- Moradi.Sepahvand, M., Amraee, T.: Integrated expansion planning of electric energy generation, transmission, and storage for handling high shares of wind and solar power generation. *Appl. Energy* 298, 117137 (2021)
- Moradi.Sepahvand, M., Amraee, T., Sadeghi.Gougheri, S.: Deep learning-based hurricane resilient co-planning of transmission lines, battery energy storages and wind farms. *IEEE Trans. Ind. Inform.* 18(3), 2120–2131 (2021)
- Luburić, Z., Pandžić, H., Carrión, M.: Transmission expansion planning model considering battery energy storage, TCSC and lines using AC OPF. *IEEE Access* 8, 203429–203439 (2020)
- Dehghan, S., Amjady, N.: Robust transmission and energy storage expansion planning in wind farm-integrated power systems considering transmission switching. *IEEE Trans. Sustainable Energy* 7(2), 765–774 (2016)
- Wang, S., Geng, G., Jiang, Q.: Robust co-planning of energy storage and transmission line with mixed integer recourse. *IEEE Trans. Power Syst.* 34(6), 4728–4738 (2019)
- Nikoobakht, A., Aghaei, J.: Integrated transmission and storage systems investment planning hosting wind power generation: continuous-time hybrid stochastic/robust optimisation. *IET Gener. Transm. Distrib.* 13(21), 4870–4879 (2019)
- Fang, B., Xie, R., Wei, W., Li, Y., Mei, S.: A distributionally robust approach for transmission and energy storage capacity planning in a remote photovoltaic power plant. In: 2020 39th Chinese Control Conference (CCC), pp. 6141–6145. IEEE, Piscataway, NJ (2020)
- Yang, L., Xie, R., Wei, W., Sun, C., Mei, S.: Coordinated planning of storage unit in a remote wind farm and grid connection line: a distributionally robust optimization approach. In: 2019 IEEE Innovative Smart Grid Technologies - Asia (ISGT Asia), pp. 424–428. IEEE, Piscataway, NJ (2019)
- Guo, Z., Wei, W., Chen, L., Xie, R., Mei, S.: Sizing energy storage to reduce renewable power curtailment considering network power flows: a distributionally robust optimisation approach. *IET Renew. Power. Gener.* 14(16), 3273–3280 (2020)
- Guo, Z., Xie, R., Ma, Q., Yang, L., Wei, W., Mei, S.: Impact of storage and transmission line capacity on the curtailment of a remote renewable plant: A multiparametric programming methods. In: 2020 10th International Conference on Power and Energy Systems (ICPES), pp. 489–492. IEEE, Piscataway, NJ (2020)
- Fernández-Blanco, R., Dvorkin, Y., Xu, B., Wang, Y., Kirschen, D.S.: Optimal energy storage siting and sizing: a WECC case study. *IEEE Trans. Sustain. Energy* 8(2), 733–743 (2017)



33. Fiorini, L., Pagani, G.A., Pelacchi, P., Poli, D., Aiello, M.: Sizing and siting of large-scale batteries in transmission grids to optimize the use of renewables. *IEEE J. Emerging Sel. Top. Circuits Syst.* 7(2), 285–294 (2017)
34. Yan, S., Zheng, Y., Hill, D.J.: Frequency constrained optimal siting and sizing of energy storage. *IEEE Access* 7, 91785–91798 (2019)
35. Naidji, I., Ben.Smida, M., Khalgui, M., Bachir, A., Li, Z., Wu, N.: Efficient allocation strategy of energy storage systems in power grids considering contingencies. *IEEE Access* 7, 186378–186392 (2019)
36. Rodríguez.Gallegos, C.D., Gandhi, O., Yang, D., Alvarez.Alvarado, M.S., Zhang, W., Reindl, T., et al.: A siting and sizing optimization approach for PV-battery-diesel hybrid systems. *IEEE Trans. Ind. Appl.* 54(3), 2637–2645 (2018)
37. Lai, K., Zhang, L.: Sizing and siting of energy storage systems in a military-based vehicle-to-grid microgrid. *IEEE Trans. Ind. Appl.* 57(3), 1909–1919 (2021)
38. Gong, K., Wang, X., Jiang, C., Shahidehpour, M., Liu, X., Zhu, Z.: Security-constrained optimal sizing and siting of bess in hybrid AC/DC microgrid considering post-contingency corrective rescheduling. *IEEE Trans. Sustainable Energy* 12(4), 2110–2122 (2021)
39. Giannitrapani, A., Paoletti, S., Vicino, A., Zarrilli, D.: Optimal allocation of energy storage systems for voltage control in LV distribution networks. *IEEE Trans. Smart Grid* 8(6), 2859–2870 (2017)
40. Erdinc, O., Taşçıkaraoğlu, A., Paterakis, N.G., Dursun, I., Sinim, M.C., Catalão, J.P.S.: Comprehensive optimization model for sizing and siting of DG units, EV charging stations, and energy storage systems. *IEEE Trans. Smart Grid* 9(4), 3871–3882 (2018)
41. Novoa, L., Flores, R., Brouwer, J.: Optimal renewable generation and battery storage sizing and siting considering local transformer limits. *Appl. Energy* 256, 113926 (2019)
42. Shen, Z., Wei, W., Wu, D., Ding, T., Mei, S.: Modeling arbitrage of an energy storage unit without binary variables. *CSEE J. Power Energy Syst.* 7(1), 156–161 (2021)
43. Esfahani, P.M., Kuhn, D.: Data-driven distributionally robust optimization using the Wasserstein metric: performance guarantees and tractable reformulations. *Math. Program.* 171, 115–166 (2018)
44. Rahimian, H., Mehrotra, S.: Distributionally robust optimization: a review. *arXiv:1908.05659* (2019)
45. Delage, E., Ye, Y.: Distributionally robust optimization under moment uncertainty with application to data-driven problems. *Oper. Res.* 58(3), 595–612 (2010)
46. Popescu, I.: A semidefinite programming approach to optimal-moment bounds for convex classes of distributions. *Math. Oper. Res.* 30(3), 632–657 (2005)
47. Rockafellar, R.T., Uryasev, S.: Optimization of conditional value-at-risk. *J. Risk* 2, 21–42 (2000)
48. Nemirovski, A., Shapiro, A.: Convex approximations of chance constrained programs. *SIAM J. Optim.* 17(4), 969–996 (2006)
49. Gal, T., Nedoma, J.: Multiparametric linear programming. *Manage. Sci.* 18(7), 406–422 (1972)
50. Boyd, S., Vandenberghe, L.: *Convex Optimization*. Cambridge University Press, Cambridge (2004)
51. Konno, H.: A cutting plane algorithm for solving bilinear programs. *Math. Program.* 11, 14–27 (1976)
52. Shapiro, A., Kleywegt, A.: Minimax analysis of stochastic problems. *Optim. Methods Software* 17(3), 523–542 (2002)
53. The National Renewable Energy Laboratory: Home-NSRDB. NREL (2021). <https://nserdb.nrel.gov/>. Accessed 8 September 2021
54. Löfberg, J.: YALMIP : A toolbox for modeling and optimization in MATLAB. In: *Proceedings of the IEEE International Symposium on Computer-Aided Control System Design*, pp. 284–289. IEEE, Piscataway, NJ (2004)
55. Gurobi Optimization: Gurobi - the fastest solver - gurobi. Gurobi (2021). <http://www.gurobi.com/>. Accessed 8 September 2021
56. Zhao, C., Guan, Y.: Data-driven risk-averse two-stage stochastic program with  $\zeta$ -structure probability metrics. *Optimization Online* (2015). [http://www.optimization-online.org/DB\\_HTML/2015/07/5014.html](http://www.optimization-online.org/DB_HTML/2015/07/5014.html). Accessed 8 September 2021

**How to cite this article:** Xie, R., Wei, W., Ge, M.-F., Wu, Q., Mei, S.: Coordinate sizing of energy storage and transmission line for a remote renewable power plant. *IET Renew. Power Gener.* 16, 2508–2520 (2022). <https://doi.org/10.1049/rpg2.12440>